frontiers | Frontiers in Environmental Science

TYPE Original Research
PUBLISHED 02 May 2024
DOI 10.3389/fenvs.2024.1380979

OPEN ACCESS

EDITED BY
Xudong Huang,
North China University of Water Conservancy and Electric Power, China

REVIEWED BY
Elizabeth Graham,
University College London, United Kingdom
Zhuoran Wang,
Shandong Agricultural University, China
Zhong-Xiu Sun,
Shenyang Agricultural University, China

*CORRESPONDENCE
Wenjing Wang,
wangwenjing_2012@163.com

RECEIVED 02 February 2024
ACCEPTED 10 April 2024
PUBLISHED 02 May 2024

CITATION
Zha L, Wang W, Zhong J, Su Y and Chang D (2024), How did ancient human activities influence the properties and development of soil?—a case study of the Yangshao Village cultural relic site, Henan Province.
Front. Environ. Sci. 12:1380979.
doi: 10.3389/fenvs.2024.1380979

How did ancient human activities influence the properties and development of soil?—a case study of the Yangshao Village cultural relic site, Henan Province

Lisi Zha[1], Wenjing Wang[2,3]*, Junhong Zhong[4], Yiqi Su[5] and Dandan Chang[1]

[1]School of Public Administration, Guangdong University of Finance and Economics, Guangzhou, Guangdong Province, China, [2]School of Resource and Environmental Sciences, Hebei Normal University for Nationalities, Chengde, Hebei, China, [3]Centre for Human Sciences, Universiti Malaysia Pahang AL-Sultan Abdullah, Kuantan, Malaysia, [4]Guangdong University of Technology, Guangzhou, Guangdong Province, China, [5]Jinan University, Guangzhou, Guangdong Province, China

Introduction: What were the effects of paleoanthropogenic activities on the physicochemical properties and degree of the development of soil? To search for this answer, we can not only understand the different types of ancient human activities but also explore the intensity and characteristics of the activities.

Methods: In this study, soil samples from different soil layers and two profiles in the Yangshao Village cultural site in Henan Province were collected. Their physicochemical properties and the sporophyte phyllosilicates they contain were analyzed and compared.

Results: We found that the paleoanthropogenic activities started in the relatively low-lying area, in which the slash-and-burn activities resulted in the soil being filled with intrusions such as charcoal debris and ceramic shards. At the same time, the coarse-grained matter was affected by the plowing activities and mostly decomposed into fine particles, and the content of clay particles reached an extreme value. The total nitrogen, phosphorus, and calcium carbonate content exceeded the average value of the natural profile, indicating that ancient humans had used human and animal feces to a certain extent to restore the fertility of arable land.

Discussion: Overall, ancient human activities hindered the development of the soil, especially the ground created due to habitation activities. From the type and content of clay minerals, it could be seen that the soil in this layer has been transported from other places, has a high content of clay particles, and has experienced fire baking. It was assumed that the ground was used to cover the grain or bury the garbage and lay with clay in order to achieve the effect of sealing. As a result, the soil voids and structure had been damaged to some extent, which prevented the downward leaching or precipitation of soil particles and minerals to a certain extent, thus affecting soil development.

KEYWORDS

Yangshao Village site, archaeological soil, soil properties, soil development, paleoenvironment

1 Introduction

In 1883, Vasily Vasilievich Dokuchaev published "Russian Chernozem," which first formally put forward the five major factors of soil formation (climate, topography, soil parent matter, biological factors, and time). This was a great achievement in the history of soil science, which had long been known to soil scientists. The impact of human activities on the soil was not taken seriously at that time. However, in the last century, human beings have been recognized as an important component of biological factors, and increasing attention has been paid to the influence of human activities on soil. In the study of archaeological soil, in 2004, a critical review of the current methods of sampling and analyzing soils for the determination of metals in archaeological prospection was presented (R. Haslam and Tibbett, 2004). During the same period, the plant physiological investigation of starch grains found as residues on artifacts and in archaeological sediments was reviewed (M. Haslam, 2004).

In 2008, soil analyses in archeology as a subject developed during the 1950s and 1960s, and the effects of human activities on soils were first investigated (Macphail, 2008). Furthermore, how soil research can reveal the impact of human activities on landscapes and spaces was described (Walkington, 2010). Soil analysis was a very useful tool to investigate the effects of human activities on soil development and burying bodies on soil contamination, raw material provenance, paleoenvironmental reconstruction, and the environmental impact of cultural heritage (Pastor et al., 2016). The types and intensities of ancient human activities can be recognized by analyzing the physical and chemical properties of soil and inclusions. A multi-element analysis of soils has been used to understand the former space use. Results from these studies indicated that activity areas can often be chemically detected and interpreted (Knudson et al., 2004; Sullivan and Kealhofer, 2004; Terry et al., 2004; Wells, 2004; Wilson et al., 2008). Specifically, in the study of ancient agricultural production and ancient human activity areas, phosphorus, carbon, and nitrogen were frequently taken into account. This method had been used for a long time and is well-developed (Schlezinger and Howes, 2000; Fernández et al., 2002; Suleimanov and Obydennova, 2006; Lu et al., 2009; Homburg and Sandor, 2011; Gerlach et al., 2012; Migliavacca et al., 2013; Salisbury, 2013; Ferro-Vázquez et al., 2014; Nielsen and Kristiansen, 2014; Adam et al., 2016). Other elements can also provide effective clues for different land use patterns and intensities of ancient humans, especially some metal elements and trace elements, through which much more detailed areas of different ancient human activities can be distinguished (Parnell et al., 2002; Wilson et al., 2008; Kamenov et al., 2009; Dirix et al., 2013; Gallello et al., 2013; Vittori Antisari et al., 2013; Zgłobicki, 2013; Cook et al., 2014; Nielsen and Kristiansen, 2014; Stinchcomb et al., 2014; Fleisher and Sulas, 2015; Turner et al., 2021). Analyzing the magnetic susceptibility of soil can help archaeologists find evidence of ancient humans using fire (Linford and Canti, 2001; Church et al., 2007; Shi et al., 2007; Brown et al., 2009; Carrancho and Villalaín, 2011; Zhang et al., 2014). In contrast, the physical properties of soil were less analyzed, such as chroma and particle composition. However, in paleoenvironmental studies, soil physical property analysis was often used (Arnaud-fassetta et al., 2000; Tsatskin and Nadel, 2003; Kidder et al., 2012; Kim et al., 2012; Sitzia et al., 2012; Blasi et al., 2013; Solís-Castillo et al., 2013; Cruz-y-Cruz et al., 2015). In addition, clay minerals were often used in the paleoenvironment as well (Dou et al., 2010; El Ouahabi et al., 2017; Manalt et al., 2001; Oonk et al., 2009; J. Wang et al., 2015; Wilson et al., 2008), while they were less used in the study of archaeological research. Ancient human activities could change the local environment, and soil physical properties and clay minerals can also reflect the influence of ancient human activities on soil.

Yangshao Village was a Neolithic site in the Yellow River Basin of China and is the namesake of the Yangshao culture. In October 1921, the Swedish geologist Antsen and the Chinese geologist Yuan Fuli carried out the first archaeological investigation and excavation and obtained a large amount of cultural relics, which confirmed that this site was a Neolithic cultural relic. According to many archaeological excavations and research, it was found that the stratigraphy of two cultures, Yangshao and Zhongyuan Longshan, with four different stages of development, was superimposed on each other, with the late Yangshao culture being the main one (Yan, 1989). The existence of a large number of ash pits and relics within the site indicated that the ancient human activities on the site were diverse and intense, and they must have left a lot of information of ancient human activities in the soil. Combined with the results of existing paleoclimatic studies, the ancient humans at this site experienced a sudden cooling event and a great flood (SHI et al., 1992; Marcott et al., 2013; Chen et al., 2015), and the culture was in the transition to the Longshan culture of the Central Plains, so the study of the soil characteristics of the site will help us understand the production and living conditions of ancient humans in the context of paleoenvironmental changes and cultural evolution.

2 Materials and methods

2.1 Experimental framework

The Yangshao Village site is located on a terrace approximately 7.5 km north of Yangshao Village, Mianchi County, Henan Province, Eastern China (Figure 1C). The site is approximately 900 m long and 300 m wide. According to the book Soil Series of China (Henan), the zonal soil is loess, which belongs to the general development of dry and semi-arid cambisols (Wu et al., 2019). The sampling area is situated on a gentle slope to the east of Antesheng Road in Yangshao Village (34°48′51″N, 111°46′36″E), with an elevation of 621 m and a slope gradient of 5°–8°. The area spans approximately 160 m north to south and 80 m east to west. The current land use is pepper plantations. Due to site protection management requirements, there is no excessive artificial maintenance; pepper trees rely on natural precipitation, and from the scene full of weeds, it can be judged that there is minimal modern human interference. Based on the field conditions, the area can be divided into three regions from south to north: sparse pepper forest (I), dense pepper forest (II), and grassland (III). Soil samples were collected from one to two locations in the center of each region and at the boundaries between the regions. Additionally, sampling points were established along the north–south axis at 20 m intervals to the east and west of the central axis. In regions II and III, the sampling was mainly conducted to the east due to modern disturbances

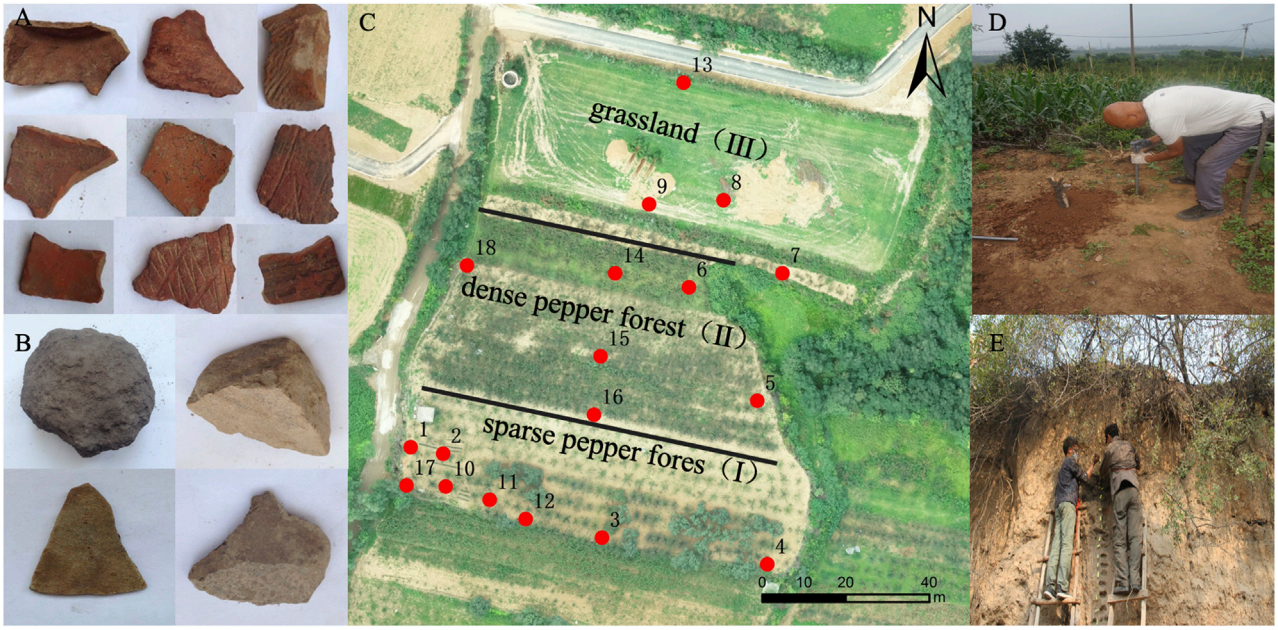

FIGURE 1
Sampling area and method.

caused by burial activities in the western region, which was identified as a burial area by the Henan Provincial Institute of Cultural Relics Research in 1981. Within region I, location Nos 1, 2, 10, 11, and 17 were previously excavated, particularly at location No. 17, where a large number of pottery shards (Figure 1A) and stone tools (Figure 1B) were found in the cultural layer. Therefore, this region was densely sampled to obtain more information of ancient cultivation activities. Location No. 18 is a natural soil profile, which was taken for comparative analysis. Soil samples were collected using soil augers at locations Nos 1 to 16, reaching the paleosol layer from the surface. Based on the soil texture and color, combined with stratigraphic dating, the soil was divided into several layers, and intact samples were collected from each layer (Figure 1D). A total of 49 samples were obtained for N, P, and CaO analysis and field observations. At location Nos 17 and 18, samples were taken directly from the profile by scraping the surface to obtain samples at a 10 cm interval, and 80 samples were taken (Figure 1E), including samples of spore pollen, phytolith, and conventional physical and chemical analysis samples.

2.2 Dating and analytical methods

The dating samples were taken according to the occurrence layer, and soil samples were collected from the bottom of each layer. However, for the cultural profile, due to human interference, although the soil layer is spatially continuous, the age would be broken, so samples were also collected from the top of some occurrence layers. In addition, some special soil layers formed by ancient human interference were also sampled and analyzed to have a clear understanding of the age sequence of the profile. Four samples were collected from the natural profile, and eight samples were collected from the cultural profile, totaling 12 samples, all of which were valid for analysis. The dating of the soil samples was carried out using the carbon-14 accelerated mass spectrometer (AMS) method, which was completed in the Laboratory of Archaeological Chronology, School of Archeology and Letters and Museums, Peking University. The 14C half-life used was 5,568 years, and B.P. is dated to 1950. The measured ages were corrected to calendar ages using the tree-wheel correction method provided by Reimer et al. (Paula et al., 2004), the curve used for the correction was IntCal04, and the program used was OxCal v3.10. Soil samples from the natural profile at 40, 220, 300, and 400 cm were measured. The results were 4,055, 5,583, 6,898 and 10,248 a B.P., respectively. Soil samples from the cultural profile at 20, 70, 100, 145, 160, 210, 230, and 400 cm were measured. The results were 3,641, 4,891, 5,531, 27,789, 6,400, 7,524, 8,241, and 12,800 a B.P., respectively. Based on the dating results, it was roughly known that culture layer 1 was formed during the Central Longshan Culture, the ash layer was formed in the late Yangshao period, culture layer 2 was formed during the middle Yangshao culture, and culture layer 3 was formed during the early Yangshao culture. According to the dating results of the two profiles, it can be roughly known from the chronological point of view that the two paleosoil layers corresponded well, the transition layer of the natural profile roughly corresponded to culture layer 3 of the culture profile, and the loess layer of the natural profile roughly corresponded to culture layers 2 and 1.

Clay minerals were identified by X-ray diffractograms. Particle size analysis was carried out using the Mastersizer 2000 laser particle sizer, magnetic susceptibility analysis was carried out using the Bartington MS-2 dual-frequency magnetic susceptibility meter, and total mineral content analysis was carried out based on ICP-AES. The spore powder was extracted via acid–base treatment,

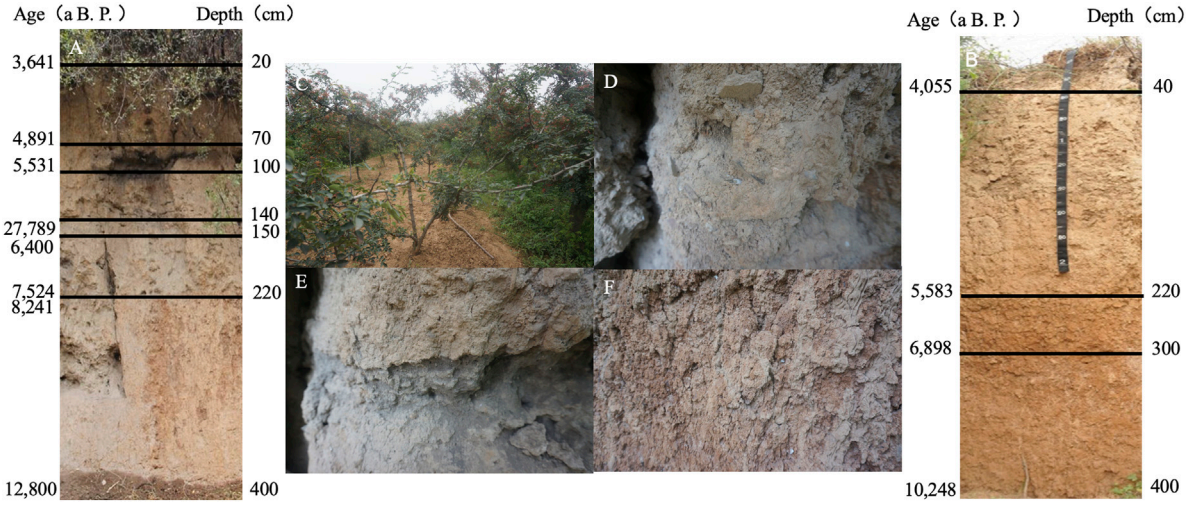

FIGURE 2
Soil profile and stratification.

heavy liquid flotation, and sieving, and the identification and counting were carried out under a Leica biomicroscope (magnification of ×400). Charcoal debris were identified and counted under a Nissan Olympus BX-51 optical microscope (magnification ×400), and charcoal debris with a diameter greater than 50 μm were counted. In addition, phyllosilicate analysis was carried out on the soil layers disturbed by paleoanthropogenic activities in the cultural profile. The phyllosilicate was separated and extracted with reference to the wet gray image method, and the extracted phyllosilicate was made into a fixation slice using neutral gum and observed, counted, and micrographically photographed under a Leica biomicroscope (magnification of × 400); its identification and classification were referred to in the relevant literature (Peninsula, 1983; Fredlund and Tieszen, 1994; Kelly et al., 1998), and the nomenclature was based on international rules (Neumann et al., 2019).

3 Result

3.1 Basic physical and chemical characteristics of soil profiles and soil columns

The soil profile at locations No. 17 (Figure 2A) and 18 (Figure 2B) exhibited distinct macroscopic differences in each layer. In order to reflect the soil characteristics of the site, combined with the classification of archaeological soil layers according to color, structure, tightness, and inter-layer contact relationship, the cultural profile can be divided from top to bottom into seven layers (Table 1). Among them, the ash layer was the remains of ancient human fire, and the cultural layer was the remains of ancient human habitation; both of them are horizontally distributed, the boundary shape was flat and regular, and in both of them, the Yangshao period red and gray ceramic tablets of the Longshan culture period of the Central Plains were found. The conical ash pits next to them are the pits dug for ancient human life garbage or food reserves, which can prove that the ash and cultural layers are the remains of ancient human activities. The topsoil layer was mostly brown, and the texture was loamy soil (Figure 2C); the cultural layer was mostly gray-brown, and the texture was powdery loam, which contained many kinds of intruders such as pottery shards and bones (Figure 2D) or special materials such as charcoal chips (Figure 2E). The paleosoil layer was turbid orange, and the texture was clay loam (Figure 2F). The entire profile was clearly layered. The natural profile is untouched by traces of disturbance, and it is divided into four layers according to the color, structure, tightness, and interlayer contact relationship. The specific descriptions of the various layers are detailed in Table 1. The average total nitrogen, phosphorus, and calcium carbonate content of the cultural profile were 0.98, 2.83, and 108.43 g kg^{-1}, respectively, while those of the natural profile were 0.57, 1.94, and 85.5 g kg^{-1}, respectively.

From locations No. 1 to 16, the soil column sampling points can also be divided into topsoil, cultural layer, and paleosol layer. Overall, the average thickness of the topsoil was 72 cm, with a dry color, mainly brown. The cultural layer had an average thickness of 112 cm, and no traces of modern human activity interference or modern intrusions were found during on-site excavation. Its dry color was mainly grayish-brown. The paleosol layer had a dry color, mainly turbid orange, which was noticeably different from the previous two layers. The soil structure of each layer was granular, while the structures at locations No. 5 and 10 were plate-like, suggesting human or fluvial deposition. Intrusions mainly consist of pottery shards and stone tools, indicating the cultural characteristics of that period. Additionally, the presence of charcoal fragments indicated the use of fire by the ancient people. The average total nitrogen content at location No. 16 is 0.87 g kg^{-1} in the topsoil, 0.85 g kg^{-1} in the cultural layer, and 0.56 g kg^{-1} in the paleosol layer. The average total phosphorus content is 1.62 g kg^{-1} in the topsoil, 2.93 g kg^{-1} in the cultural layer, and 1.31 g kg^{-1} in the paleosol layer. The average carbonate

10.3389/fenvs.2024.1380979

TABLE 1 Field description and chemical analysis of each soil layer.

Sampling	Layer and depth (cm)	Dry color	Texture	Intruder	N ($g \cdot kg^{-1}$)	P ($g \cdot kg^{-1}$)	$CaCO_3$ ($g \cdot kg^{-1}$)
1	Topsoil layer (0–80 cm)	Brown (7.5 YR 4/3)	Loam		0.91	1.71	80
	Topsoil layer (80–100 cm)	White (7.5 YR 8/1)	Silt loam		0.53	1.46	75
	Culture layer (100–250 cm)	Grayish brown (7.5 YR 4/2)	Silt loam	Black potsherd	0.46	4.52	129
	Culture layer (250–285 cm)	Cloudy yellow (10 YR 7/2.5)	Silt loam	Charcoal crumbs	0.52	1.67	128
	Culture layer (285–290 cm)	Cloudy orange (10 YR 7/3)	Silt loam		0.53	3.38	122
	Culture layer (290–320 cm)	White (7.5 YR 8/1)	Silt loam		0.51	1.66	112
	Paleosoil layer (320 cm~)	Cloudy orange (7.5 YR 6/4)	Clay loam		0.52	1.51	55
2	Culture 9 (0–80 cm)	Brown (7.5 YR 4/3)	Loam	Red and gray potsherd and charcoal crumbs	0.62	1.62	81
	Culture layer (80–230 cm)	Light brown (7.5 YR 7/2)	Silt loam		0.58	3.76	105
	Culture layer (230–280 cm)	Grayish brown (7.5 YR 4/2)	Silt loam	Bone and black and red potsherd	0.58	2.95	122
	Paleosoil layer (280 cm~)	Cloudy orange (7.5 YR 6/4)	Clay loam		0.47	1.85	53
3	Topsoil layer (0–50 cm)	Brown (7.5 YR 4/3)	Loam		1.12	1.01	52
	Paleosoil layer (50 cm~)	Cloudy orange (7.5 YR 6/4)	Clay loam		0.42	1.53	88
4	Topsoil layer (0–120 cm)	Brown (7.5 YR 4/3)	Loam		0.94	1.64	80
	Paleosoil layer (120 cm~)	Cloudy orange (7.5 YR 6/4)	Clay loam		0.44	1.85	90
5	Topsoil layer (0–60 cm)	Brown (7.5 YR 4/3)	Loam		0.87	1.55	80
	Culture layer (60–170 cm)	Cloudy yellow (10 YR 6.5/3)	Silt loam	Red potsherd	0.56	2.33	115
	Paleosoil layer (170 cm~)	Cloudy orange (7.5 YR 6/4)	Clay loam		0.52	1.46	48
6	Topsoil layer (0–100 cm)	Brown (7.5 YR 4/3)	Loam		0.71	1.51	91
	Culture layer (100–120 cm)	Light brown (7.5 YR 7/2)	Silt loam	Gray potsherd	0.56	2.17	105
	Paleosoil layer (120 cm~)	Cloudy orange (7.5 YR 6/4 (	Clay loam		0.66	0.84	64
7	Topsoil layer (0–55 cm)	Brown (7.5 YR 4/3)	Loam		0.54	1.61	88
	Culture layer (55–80 cm)	Cloudy yellow–orange (10 Y 7/2.5)	Silt loam	Gravel	0.5	2.44	129
	Culture layer (80–210 cm)	Grayish brown (7.5YR 4/2)	Silt loam		0.53	2.93	121
	Paleosoil layer (210 cm~)	Cloudy orange (7.5 YR 6/4	Clay loam		0.75	0.96	62
8	Topsoil layer (0–30 cm)	Brown (7.5 YR 4/3)	Loam		0.82	1.53	96

(Continued on following page)

TABLE 1 (*Continued*) Field description and chemical analysis of each soil layer.

Sampling	Layer and depth (cm)	Dry color	Texture	Intruder	N ($g \cdot kg^{-1}$)	P ($g \cdot kg^{-1}$)	$CaCO_3$ ($g \cdot kg^{-1}$)
	Paleosoil layer (30 cm~)	Cloudy orange (7.5 YR 6/4)	Clay loam		0.74	1.13	61
9	Topsoil layer (0–100 cm)	Brown (7.5 YR 4/3)	Loam		1.02	1.47	84
	Paleosoil layer (100 cm~)	Cloudy orange (7.5 YR 6/4)	Clay loam		0.69	0.96	70
10	Topsoil layer (0–80 cm)	Brown (7.5 YR 4/3)	Loam		1.19	1.57	75
	Culture layer (80–100 cm)	Cloudy yellow (10 YR 6.5/3)	Silt loam		0.59	1.64	73
	Culture layer (100–220 cm)	Grayish brown (7.5 YR 4/2)	Silt loam	Gravel and red and gray potsherd	0.53	3.52	134
	Culture layer (220–300 cm)	Grayish brown (7.5 YR 4/2)	Silt loam		0.52	3.59	122
	Paleosoil layer (300 cm~)	Cloudy orange (7.5 YR 6/4)	Clay loam		0.53	0.68	114
11	Topsoil layer (0–120 cm)	Brown (7.5 YR 4/3)	Loam		1.21	2.65	95
	Culture layer (120–180 cm)	Grayish brown (7.5 YR 4/2)	Silt loam	Ash	0.53	3.01	143
	Paleosoil layer (180 cm~)	Cloudy yellow–orange (10 Y 7/2.5)	Clay loam		0.81	2.64	671
12	Topsoil layer (0–60 cm)	Cloudy yellow (10 YR 6.5/3)	Loam		0.59	1.61	75
	Paleosoil layer (60 cm~)	Cloudy orange (7.5 YR 6/4)	Clay loam		0.52	1.55	55
13	Topsoil layer (0–70 cm)	Cloudy yellow (10 YR 6.5/3)	Loam		1.12	1.61	75
	Culture layer (70–120 cm)	Light brown (97.5 YR 7/2)	Silt loam	Black potsherd and red soil residue	0.55	3.99	138
	Paleosoil layer (120 cm~)	Cloudy orange (7.5 YR 6/4)	Clay loam		0.48	0.74	65
14	Topsoil layer (0–60 cm)	Brown (7.5 YR 4/3)	Loam		0.88	1.77	77
	Paleosoil layer (60 cm~)	Cloudy orange (7.5 YR 6/4)	Clay loam		0.53	1.63	62
15	Topsoil layer (0–50 cm)	Brown (7.5 YR 4/3)	Loam		0.83	1.36	76
	Paleosoil layer (50 cm~)	Cloudy orange (7.5 YR 6/4)	Clay loam		0.52	1.52	55
16	Topsoil layer (0–20 cm)	Cloudy yellow (10 YR 6.5/3)	Loam		0.53	2.64	104
	Culture layer (20–100 cm)	Cloudy orange (7.5 YR 7/3)	Silt loam	Red soil residue	0.71	2.71	109
	Paleosoil layer (100 cm~)	Cloudy orange (7.5 YR 6/4)	Clay loam		0.47	1.67	55
17	Topsoil layer (0–20)	Cloudy orange (7.5 YR 6/4)	Loam		1.11	1.51	72
	Culture layer 1 (20–70 cm)	Light brown (7.5 YR 7/2)	Silt loam	Gray potsherd	1.22	3.38	135

(Continued on following page)

10.3389/fenvs.2024.1380979

TABLE 1 (*Continued*) Field description and chemical analysis of each soil layer.

Sampling	Layer and depth (cm)	Dry color	Texture	Intruder	N ($g \cdot kg^{-1}$)	P ($g \cdot kg^{-1}$)	$CaCO_3$ ($g \cdot kg^{-1}$)
	Ash layer (70–100 cm)	Grayish brown (7.5 YR 4/2)	Silt loam	Jade rings, stoneware, and charcoal crumbs	0.71	1.15	49
	Culture layer 2 (100–140 cm)	Cloudy orange (7.5 YR 7/3)	Silt loam	Red potsherd and bone	1.01	4.76	161
	Viscosity layer (140–150 cm)	Cloudy orange (7.5 YR 6/4)	Clay loam		0.68	4.04	113
	Culture layer 3 (150–220 cm)	Cloudy orange (7.5 YR 6/4)	Silt loam	Red potsherd	1.61	4.51	166
	Paleosoil layer (220–400 cm)	Cloudy orange (7.5 YR 6/4)	Clay loam		0.56	0.47	63
18	Topsoil layer (0–20 cm)	Brown (7.5 YR 4/3)	Loam		0.75	1.65	91
	Loess layer (20–170 cm)	Light brown (7.5 YR 7/2)	Silt loam		0.51	2.10	111
	Transition layer (170–320 cm)	Grayish brown (7.5 YR 4/2)	Silt loam		0.57	2.34	78
	Paleosoil layer (255–410 cm)	Cloudy orange (7.5 YR 6/4)	Clay loam		0.43	1.66	62

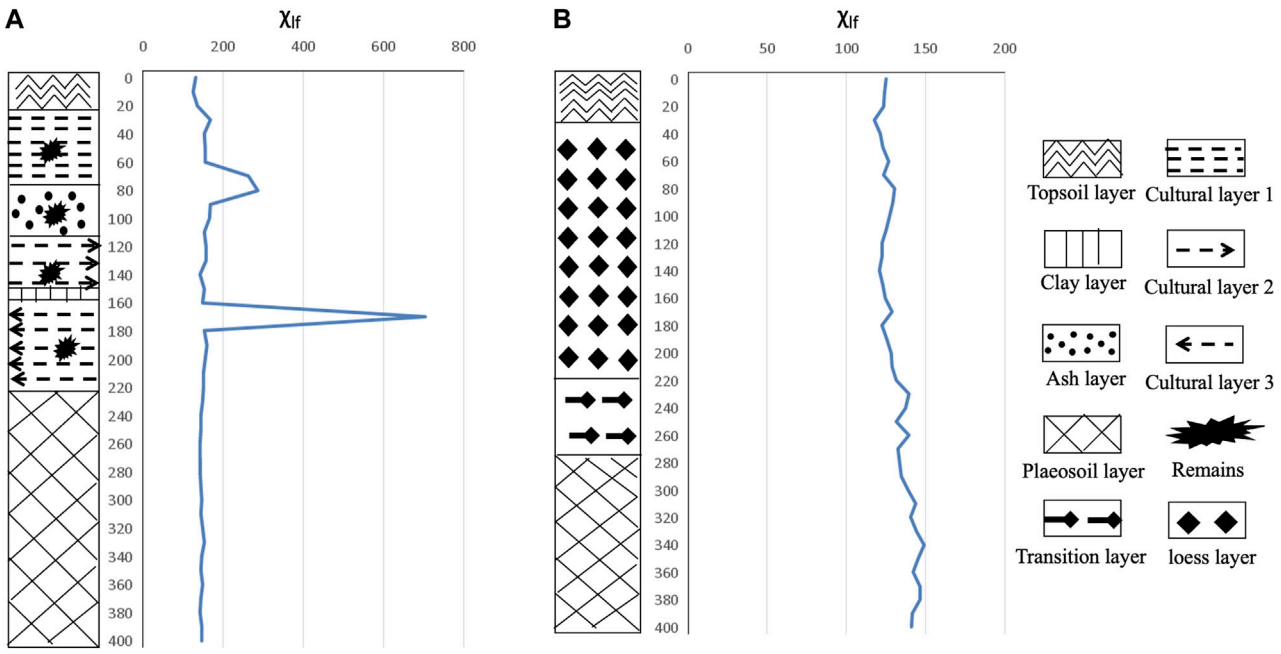

FIGURE 3
Change in the magnetic susceptibility of the natural profile.

content is 81.81 g kg^{-1} in the topsoil, 116.59 g kg^{-1} in the cultural layer, and 64.25 g kg^{-1} in the paleosol layer. Overall, the total nitrogen content is the highest in the topsoil and decreases with depth, but there are peak values in certain cultural layers. The total phosphorus and carbonate contents increase with depth, reaching the highest values in the cultural layer and decreasing to the lowest values in the paleosol layer. For more detailed information, refer to Table 1.

3.2 Magnetic susceptibility

The magnetic susceptibility data χ_{lf} in the cultural profile generally ranged from 131.67 to 705.51*10^{-8} m^3 kg^{-1}, with an average of 174.13*10^{-8} m^3 kg^{-1}. Figure 3A shows the change in magnetic susceptibility in the cultural profile. χ_{lf} showed extreme values in both the ash and cultural layers, especially reaching the maximum at 170 cm, well above the maximum of the natural profile.

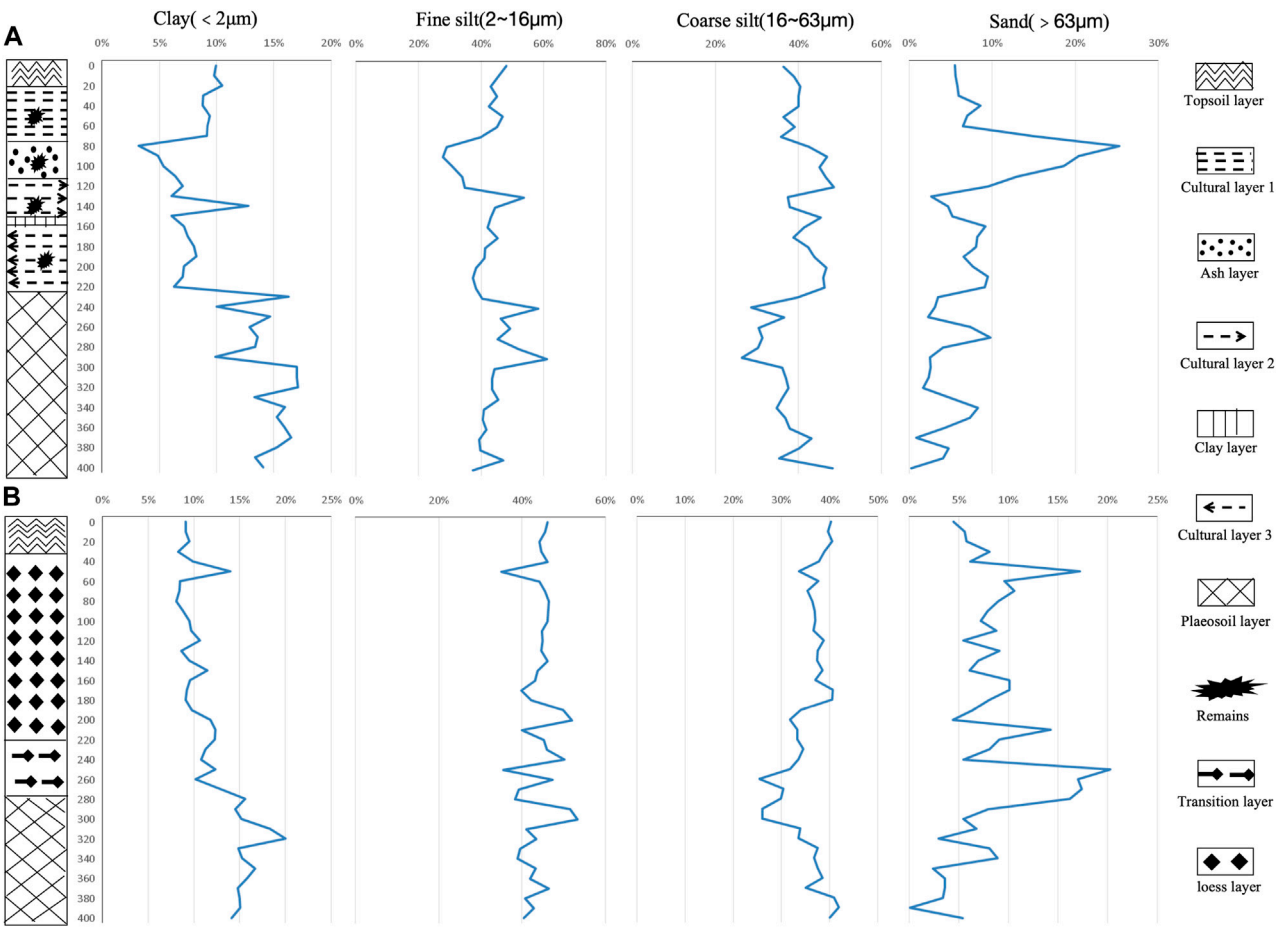

FIGURE 4
Change in the particle size of cultural and natural profiles.

The magnetic susceptibility data χ_{lf} in the natural profile generally ranged from 120.67 to 149.09 $*10^{-8}$ m^3 kg^{-1}, with an average of 132.11$*10^{-8}$ m^3 kg^{-1}. Figure 3B shows the change in magnetic susceptibility in the natural profile, where the value of χ_{lf} generally decreased with depth.

3.3 Particle size

Particle size data in the cultural profile generally averaged 10.74% for clay, 39.59% for fines, 36.30% for coarser sands, and 14.13% for sands. Figure 4A shows the change in particle size in the cultural profile, where the content of clay and fine silt increased with depth, while coarse silt and sand decreased.

The grain size data for the natural profiles averaged 11.97% for clay, 44.09% for fine chalky sand, 35.79% for coarse chalky sand, and 8.15% for sand. Figure 4B shows the change in particle size in the natural profile, where the content of clay increased with depth, while sand decreased, and fine silt and coarse sand fluctuated greatly.

In the ash layer, the sand content reached the highest value, which was much higher than the maximum value of the natural profile, while the clay content reached the lowest value, which was lower than the minimum value of the natural profile. In the culture layer, the clay content reached an extreme value.

3.4 Clay mineral

In the natural profile, characteristic peaks of kaolinite and illite were detected in the paleosoil layer. The kaolinite characteristic peaks were observed at 0.72 nm and 0.36 nm, with intensities of 89.3% and 61.7%, respectively. For illite, the characteristic peaks were found at 0.50 nm and 0.34 nm, with intensities of 37.8% and 100%, respectively (Figure 5A). In the transition layer, a variety of clay mineral characteristic peaks were detected. These included kaolinite at 0.72 nm (50.5% intensity), montmorillonite at 0.50 nm (24.0% intensity), chlorite at 0.46 nm and 0.36 nm (8.8% and 41.8% intensities, respectively), and ilmenite at 0.33 nm (73.1% intensity) (Figure 5B). In the loess layer, characteristic peaks of illite and montmorillonite were identified. Illite peaks were observed at 0.50 nm and 0.34 nm, with intensities of 12.9% and 36.0%, respectively, while montmorillonite exhibited a peak at 1.48 nm, with an intensity of 36.1% (Figure 5C). In the topsoil layer, characteristic peaks of ilmenite and chlorite were detected. Ilmenite peaks were found at 1.01 nm and 0.50 nm, with intensities of 100% and

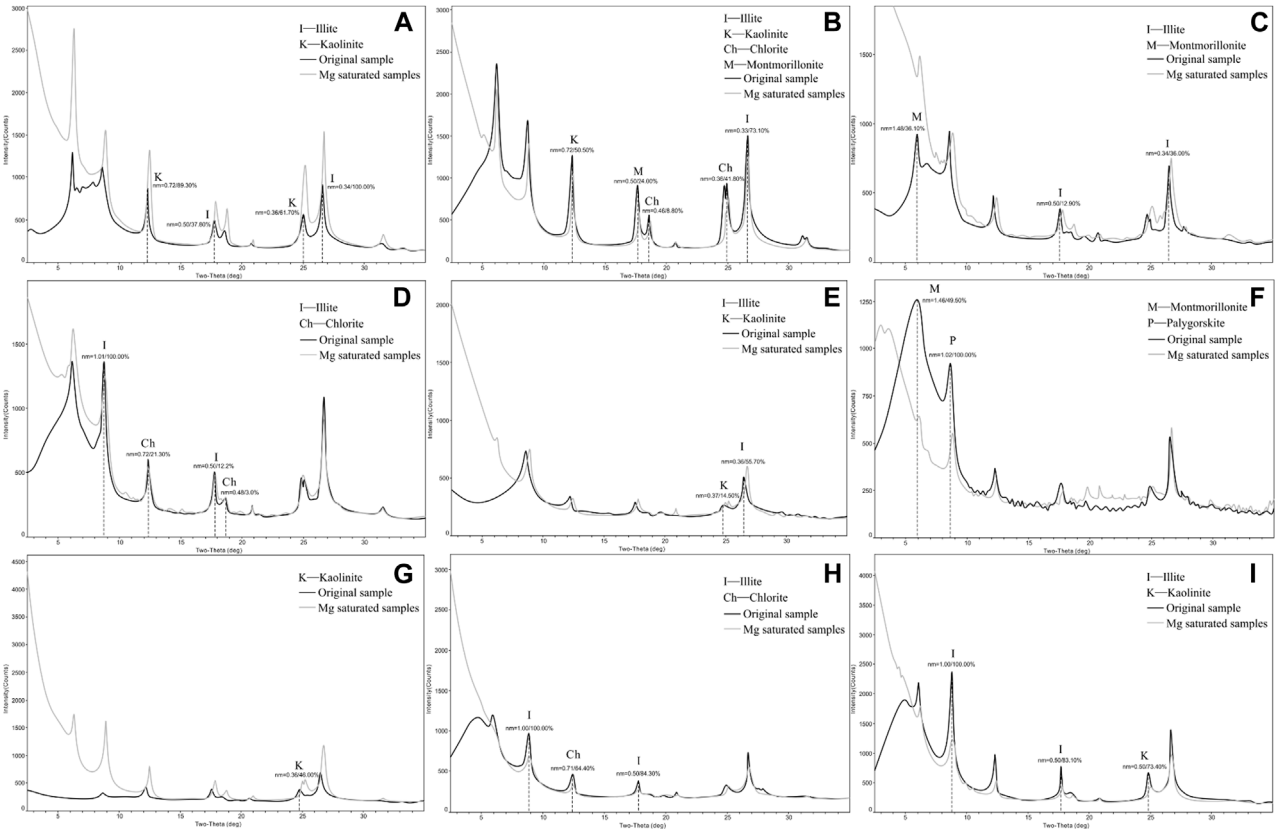

FIGURE 5
Directional map of clay minerals.

12.2%, respectively, while chlorite exhibited peaks at 0.72 nm and 0.48 nm, with intensities of 21.3% and 3.0%, respectively (Figure 5D).

In the cultural profile, characteristic peaks of kaolinite and illite were detected in the paleosoil layer, with kaolinite at 0.37 nm (intensity 14.5%) and illite at 0.36 nm (intensity 55.7%) (Figure 5E). In culture layer 3, peaks of montmorillonite and pozzolanite were identified. Montmorillonite exhibited a peak at 1.46 nm with an intensity of 49.5%, while pozzolanite showed a peak at 1.02 nm with an intensity of 100% (Figure 5F). In culture layer 2, a kaolinite peak was observed at 0.46 nm with an intensity of 46%, and it exhibited an un-sharp peak shape (Figure 5G). In culture layer 1, characteristic peaks of illite and chlorite were detected. Illite peaks were found at 1.00 and 0.50 nm, with intensities of 100% and 84.3%, respectively, while chlorite exhibited a peak at 0.71 nm, with an intensity of 64.4% (Figure 5H). In the topsoil layer, characteristic peaks of illite and kaolinite were observed. Illite peaks were detected at 1.00 and 0.50 nm, with intensities of 100% and 83.1%, respectively, while kaolinite exhibited a peak at 0.50 nm, with an intensity of 73.4% (Figure 5I).

3.5 Soil development indexes

The cultural profile development indexes Sa, Saf, and ba ranged from 7.63 to 10.94, 14.19 to 20.35, and 0.18 to 0.29, respectively, and the change rule of the three values was the same (Figure 6A). In the topsoil layer, there was almost no change in the three, with mean values of 8.73, 16.30, and 0.22, respectively. In culture layer 1, the values of the three increased slightly with depth, with mean values of 8.82, 16.46, and 0.23, respectively. Since the ash layer is no longer a general soil material due to the foreign materials added by ancient humans, its development indicator values are not significant. In culture layer 2, the values of the three increased significantly with depth, and the average values of the three were 8.80, 16.48, and 0.23, respectively. In culture layer 3, the three values have no change, and the average values of the three are 8.78, 16.38, and 0.22, respectively. In the paleosol, the three values increased slightly with depth, reached a peak at 350 cm, and an anomalous peak appeared at 270 cm, indicating that the soil development experienced strong anomalous environmental effects, and then began to decrease slightly, with the three average values of 8.02, 15.01, and 0.19, respectively.

The natural profile development indexes Sa, Saf, and ba ranged from 6.98 to 8.64, 12.96 to 16.25, and 0.15 to 0.23, respectively, and the change pattern of the three values was the same (Figure 6B). In the loess layer, the three values increased with depth while slightly fluctuating, and they reached the maximum value at the bottom; however, at 130 cm, there was an abnormal trough, and the average values of the three values were 8.26, 15.71, and 0.21, respectively. In the transition layer, the three values decreased with depth, in which the changes in Sa and Saf values fluctuated slightly, and the average values of the three were 8.18, 15.45, and 0.20, respectively. In the paleosol layer, the three values increased with depth, and at 270 cm,

10.3389/fenvs.2024.1380979

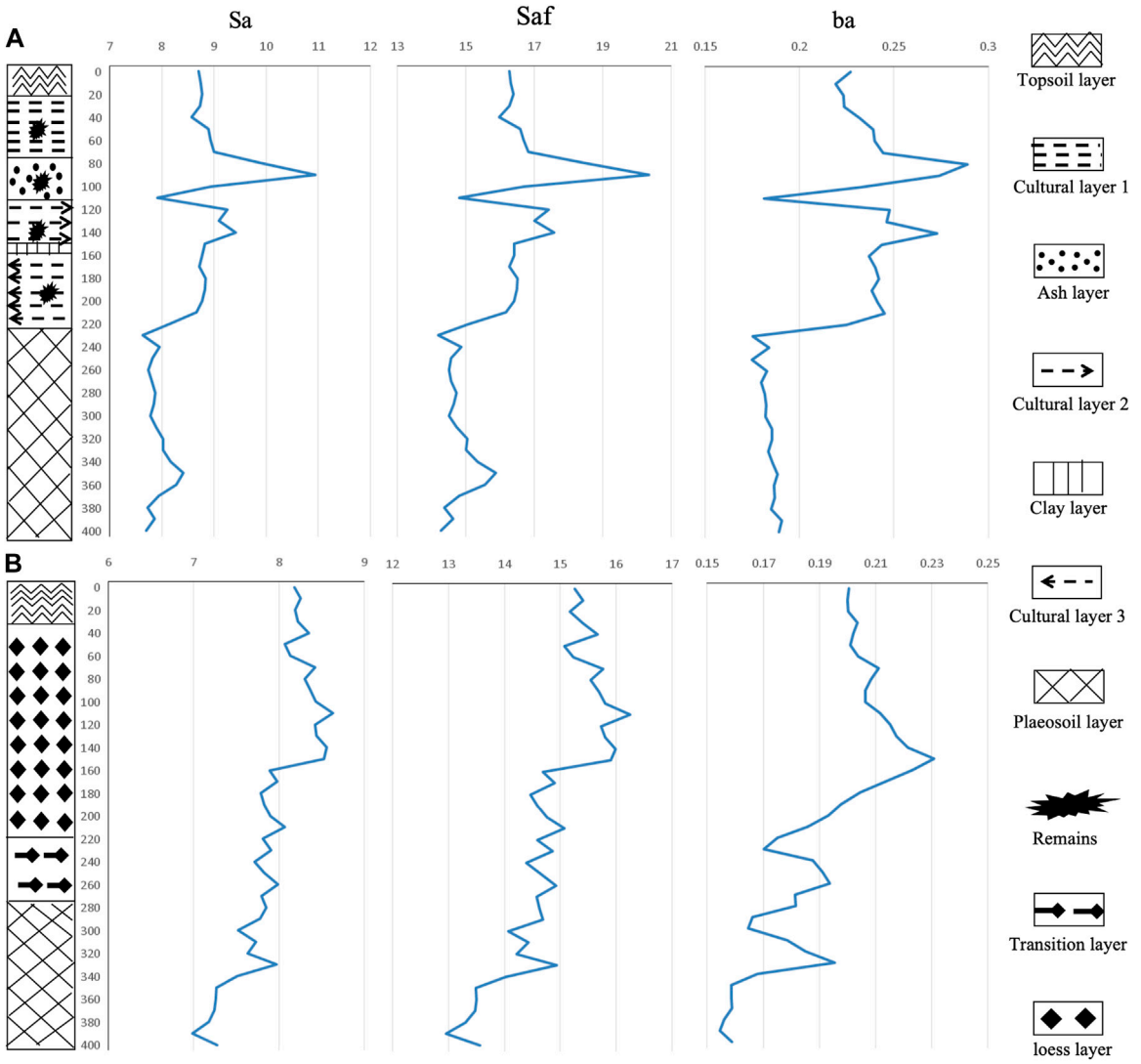

FIGURE 6
Change in the soil development indexes of cultural and natural profiles.

there was an anomalous peak, and the average values of the three values were 8.01, 14.97, and 0.19, respectively.

It can be seen that the degree of development of the cultural and natural profiles increases with depth, reaching a maximum in the paleosols, and at this point, both the developmental indicators have similar values, suggesting that both have similar environmental contexts.

3.6 Spore pollen and charcoal

The typical spore and pollen images identified are shown in Figure 7. The percentage content of pollen in the cultural profile samples was mainly composed of herbaceous plant pollen, indicating a temperate grassland vegetation landscape at that time. The identified herbaceous plant pollen was mainly composed of Gramineae, Chenopodiaceae, and Artemisia, with content changes ranging from 3.50% to 72.64%, 1.49% to 32.81%, and 4.37% to 61.39%, and the average values were 24.81%, 9.43%, and 37.85%, respectively. In addition, it was found that pollen from woody plants appeared in most layers, with Castanea, Juglans, Carpinus, Betula, Quercus, and Pinus being the main pollen species, with the content of 0%–2.70%, 0%–2.13%, 0%–4.90%, 0%–4.35%, 0%–1.50%, and 0%–10.53%, and the average values were 0.58%, 0.57%, 0.91%, 1.50%, 4.39%, and 3.09%, respectively. *Fern* pollen mainly appeared in the upper part of the cultural profile and rarely in other layers. The content changes from 0% to 20.56%, with an average value of 2.69%. The concentration value of carbon chips identified and counted ranged from 548 to 438,152 particles/g, with an average value of 57,931 particles/g.

The percentage of the pollen content in the natural profile samples was also mainly composed of herbaceous plant pollen. The identified grass pollen was mainly composed of Gramineae, Chenopodiaceae, and Artemisia pollen, whose content ranged from 1.46% to 24.41%, 2.50% to 20.28%, and 3.47% to 78.00%, and the

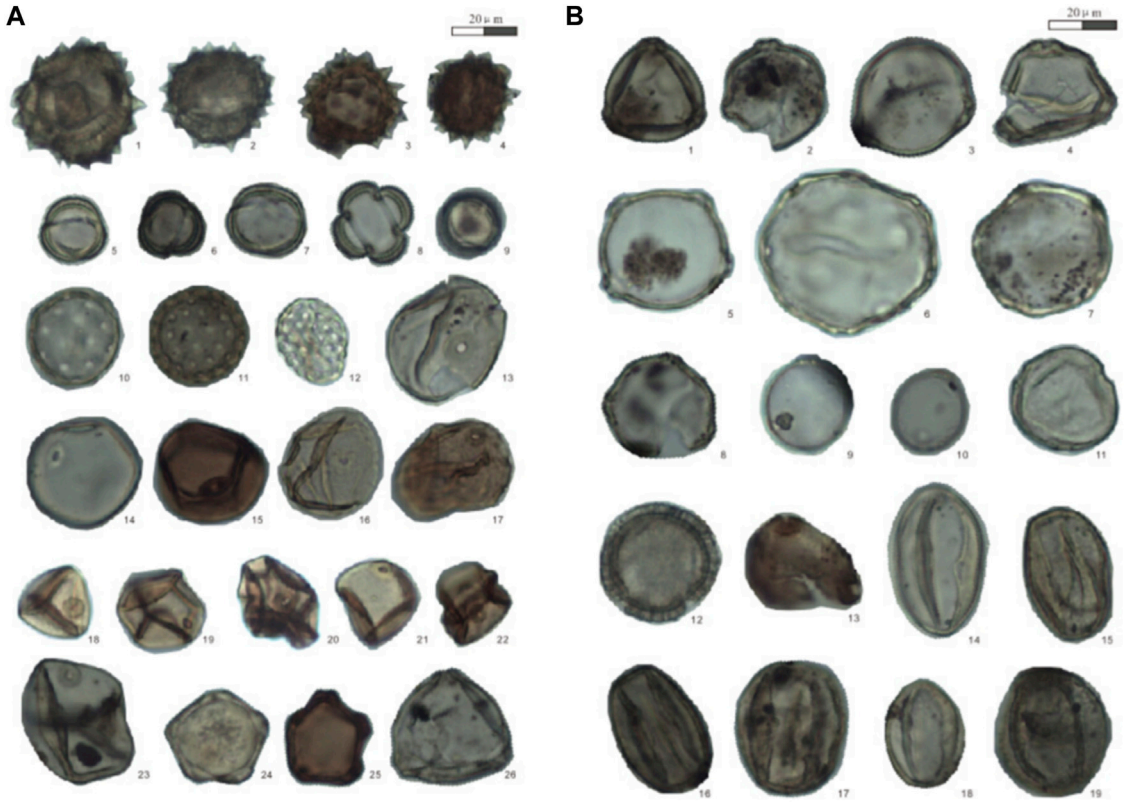

FIGURE 7
Pollen plate 1 **(A)** and plate 2 **(B)** (A: 1–4. Compositae; 5–9. Artemisia; 10–12. Chenopodiaceae; 13–23. Gramineae; 24–25. Alnus; and 26. Corylus; **(B)** 1–4. Betula; 5. Carpinus; 6. Juglans; 7. Pterocarya; 8. Carpinus; 9–10. Humulus; 11. Carya; 12. Polygonum; 13. Tilia; and 14–19. Quercus).

average values were 9.69%, 7.45%, and 41.02%, respectively. In addition, it was found that woody plant pollen appeared in most layers, with the main pollen being Castanea, Juglans, Carpinus, Betula, Quercus, and Pinus, whose content varied from 0% to 1.03%, 0% to 1.74%, 0% to 20.45%, 0% to 5.58%, 0% to 8.02%, and 0.94% to 6.90%, with an average of 0.38%, 0.43%, 2.25%, 1.13%, 3.35%, and 2.74%, respectively. The pollen of ferns mainly appears in the upper part of the natural section, and it rarely appears in the other layers. The variation range was 0%–46.50%, with an average value of 12.63%. The concentration value of carbon chips identified and counted ranges from 829 to 106,376 particles/g, with an average value of 14,394 particles/g.

3.7 Phytolith

More than 20 typical types of phytoliths were found in the cultural profile, with the main ones being rod type, dumbbell type, cross type, duct type, fan type, and square type. Among these types, crop phytoliths such as millet and rice were also found (Figure 8). Among them, the identified millet and millet-type phytoliths all came from the lemma shell of the seeds, while the identified rice phytoliths mainly came from the fan-shaped and side-by-side dumbbell-shaped stem and leaf tissues. The vast majority of the phytolith types identified in all samples were Gramineae, with dumbbell- and rod-shaped ones being the main types.

4 Discussion

4.1 Impact of soil physical and chemical properties

From the analysis of the surface data of the whole study area and based on the thickness data of paleosoil, cultural, and topsoil layers at 18 locations, the kriging interpolation method and ContextCapture software were used to generate the three-dimensional model of each soil layer. Combined with the results of paleoclimate research at the site (ZHA et al., 2020), the climate warmed and turned stable, warm, and humid after entering the Holocene, corresponding to the paleosoil layer (Figure 9A). Ancient humans started their activities in the relatively low-lying areas I and III, and the soil layer began to accumulate to form a cultural layer (Figure 9B), which contained a cultivation layer, especially in area I, where the low-lying area was convenient for irrigation and was super-southern, with sufficient light, making it easy to carry out agricultural activities. Most researchers believed that agriculture in the Yangshao culture in the Central Plains was practiced in the form of shifting cultivation, which was cultivating a plot of land for a period of time and then transferring it to a new plot of land to cultivate crops when the fertility of the land was depleted. The expansion of new plots of land was generally believed to be through the "slash-and-burn" method (Chang, 1967; Li, 1980; An, 1988). Slash-and-burn cultivation led the soil to be filled with charcoal

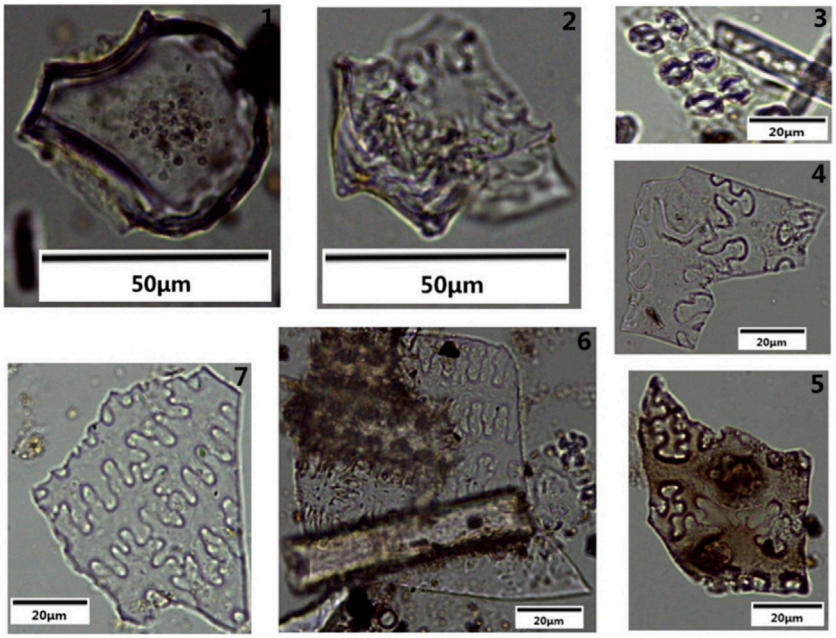

FIGURE 8
Main types of agricultural phytolith in the cultural site (1. rice fan-shaped; 2. rice bimodal; 3. rice side-by-side dumbbell-shaped; 4–5. corn husk Ω-type; 6–7. millet glume η-type).

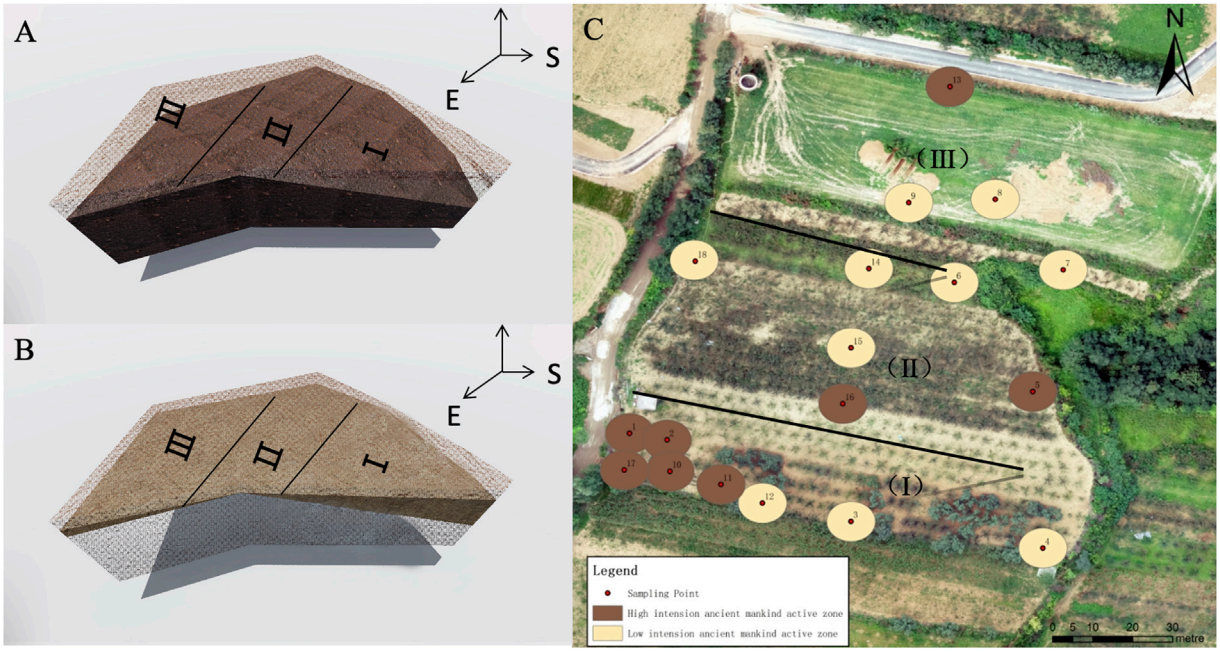

FIGURE 9
Probability area of ancient farming.

debris and other intruders, and therefore, the magnetization value was outside the extreme range. At the same time, the coarse-grained matter was affected by the plowing activities and decomposed into fine particles with a high content of sticky particles.

Combining the results of the macro-observation and basic physicochemical analysis of soil at each sampling point, there was a good correspondence between them, and the probability of ancient farming activities can be divided into two categories: high

TABLE 2 Main soil characteristics and ancient tillage probability at various locations.

Sample point	Macroscopic observation	Basic physical and chemical analysis	Ancient probability of tillage
1	Black pottery flakes and charcoal	T(N) < $\overline{X(N)}$,T(P) > $\overline{X(P)}$, and T (Ca) > $\overline{X(Ca)}$	High
2	Calcium carbonate nodules, red-black gray pottery, charcoal, and bones	T(N) < $\overline{X(N)}$, T(P) > $\overline{X(P)}$, and T (Ca) > $\overline{X(Ca)}$	High
3	No traces of artificial disturbance	T(N) > $\overline{X(N)}$ T(P) < $\overline{X(P)}$, and T (Ca) < $\overline{X(Ca)}$	Low
4	No traces of artificial disturbance	T(N) > $\overline{X(N)}$,T(P) < $\overline{X(P)}$, and T (Ca) < $\overline{X(Ca)}$	Low
5	Soil structure sheet and red pottery	T(N) > $\overline{X(N)}$,T(P) < $\overline{X(P)}$, and T (Ca) < $\overline{X(Ca)}$	Low
6	Gray pottery	T(N)> $\overline{X(N)}$,T(P) < $\overline{X(P)}$, and T (Ca) > $\overline{X(Ca)}$	Low
7	No traces of artificial disturbance	T(N) > $\overline{X(N)}$, T(P) ≈ $\overline{X(P)}$, and T (Ca) > $\overline{X(Ca)}$	Low
8	No traces of artificial disturbance	T(N) > $\overline{X(N)}$, T(P) < $\overline{X(P)}$, and T (Ca) < $\overline{X(Ca)}$	Low
9	No traces of artificial disturbance	T(N) > $\overline{X(N)}$, T(P) < $\overline{X(P)}$, and T (Ca) < $\overline{X(Ca)}$	Low
10	Flaky calcium carbonate nodules, red ash pottery, and gravel	T(N) > $\overline{X(N)}$, T(P) > $\overline{X(P)}$, and T (Ca) > $\overline{X(Ca)}$	High
11	Carbon chips	T(N) > $\overline{X(N)}$,T(P) > $\overline{X(P)}$, and T (Ca) > $\overline{X(Ca)}$	High
12	No traces of artificial disturbance	T(N) < $\overline{X(N)}$, T(P) < $\overline{X(P)}$, and T (Ca) < $\overline{X(Ca)}$	Low
13	Black pottery and red soil slag	T(N) > $\overline{X(N)}$,T(P) > $\overline{X(P)}$, and T (Ca) > $\overline{X(Ca)}$	High
14	No traces of artificial disturbance	T(N) > $\overline{X(N)}$, T(P) < $\overline{X(P)}$, and T (Ca) < $\overline{X(Ca)}$	Low
15	No traces of artificial disturbance	T(N) > $\overline{X(N)}$ T(P) < $\overline{X(P)}$, and T (Ca) < $\overline{X(Ca)}$	Low
16	Red soil slag	T(N) ≈ $\overline{X(N)}$, T(P) > $\overline{X(P)}$, and T (Ca) > $\overline{X(Ca)}$	High
17	Crumb granular, red ash pottery, jade ring, stone, bone, and charcoal	T(N) > $\overline{X(N)}$ T(P) > $\overline{X(P)}$, and T (Ca) > $\overline{X(Ca)}$	High
18	No traces of artificial disturbance	T(N) < $\overline{X(N)}$, T(P) < $\overline{X(P)}$, and T (Ca) < $\overline{X(Ca)}$	low

and low, as shown in Table 2. The high-probability sample points mostly showed the presence of artifact intrusions, such as pottery shards and charcoal chips, and the total nitrogen, phosphorus, and calcium carbonate content exceeded the average value of the natural profile. This is not only consistent with the study of agriculture in the Central Plains of the Yangshao culture but also with the study of prehistoric rice soils in the south, as well as the results of the international study of ancient dryland soils, which indicated that ancient humans used human and animal feces to a certain extent to restore the fertility of arable land (Cao et al., 2007; Dahms, 1998; X; Wang et al., 2018; Zhong and Zhao, 2023). The probability space distribution is shown in Figure 9C.

In addition, the speculation about farming activities was also confirmed by comparing the sporoderm content and the species of the cultural and natural profiles (Table 3). It was found that the concentration of pollen in the dense samples of the cultural profile was significantly higher than that of the natural profile, and it was observed that the content of Gramineae varied most obviously, the average content of the cultural profile was about three times that of the natural profile, and the crop phytosilicates of maize, millet, and rice that were identified belonged to the Gramineae group of plants. In addition to Gramineae, the content of *Quinoa* in the cultural profile is also significantly higher than that in the natural profile, and spinach, thick-skinned lettuce, sugar beet, and pigweed in the *Quinoa* family were all available for human consumption. Other major species and genera identified, such as Artemisia, Artocarpus, Selaginella, and other non-food crops, were found in large quantities in the natural profiles, and their contents were much higher than those in the cultural profiles. This indicated that when ancient human activities began to enhance, the ancient humans

TABLE 3 Comparison of sporopollen and charcoal between the cultural and natural profiles.

	Cultural profile			Natural profile		
	Maximum value	Minimum value	Mean value	Maximum value	Minimum value	Mean value
Concentration of spore powder (grain/g)	1,570.55	7.83	247.99	902.07	1.65	160.86
Concentration of charcoal dust (grains/g)	438,152.87	548.23	57,931.44	106,376.29	828.80	14,394.43
A/C	10.33	0.50	4.55	31.20	0.58	6.82
Herbaceous proportion (%)	96.02	67.29	84.43	95.69	38.00	71.98
Woody proportion (%)	23.76	3.98	12.04	30.30	4.31	12.09
Proportion of ferns (%)	21.96	0.00	3.53	46.50	0.00	15.94
Broad-leaved woody pollen content (%)	18.32	2.91	9.46	25.00	2.44	8.96
Warm-loving pollen content (%)	4.74	0.00	1.41	4.78	0.00	1.40
Cyclophyllum concentration (grains/g)	125.64	0.00	10.03	319.79	0.00	45.44
Cyclophyllum/spore pollen	3.39	0.00	0.22	8.30	0.00	0.73
AP/NAP	0.29	0.04	0.15	0.73	0.05	0.20
Artemisia (%)	61.39	4.37	37.85	78.00	3.47	41.02
Compositae (%)	9.00	0.00	2.70	21.05	0.47	4.68
Chenopodiaceae (%)	32.81	1.49	9.43	20.28	2.50	7.45
Carpinus (%)	4.90	0.00	0.95	20.45	0.00	2.25
Gramineae (%)	72.64	3.50	24.81	24.41	1.46	9.69
Quercus (%)	10.50	0.00	4.39	8.02	0.00	3.35
Selaginella (%)	5.14	0.00	0.50	43.00	0.00	4.37

selectively planted and harvested the plants needed for survival and living, resulting in an obvious increase in the content of Gramineae and *Quinoa*, while the plants with little utilization value were cut down and burned due to the needs of habitation and cultivation, which led to a decrease in the content of woody and fern-like plants.

From the point data analysis of the two typical profiles, the ratio of the average contents of clay, fine silt, coarse silt, and sand between the cultural and natural profiles is 0.91, 0.95, 1.01, and 1.38, respectively, and the ratio of the coefficient of variation is 1.50, 1.59, 0.98, and 1.25, respectively, which shows that the degree of change in the particle size of the cultural profile is greater than that of the natural profile, and the change in the clay particle is especially obvious. In addition, the particle size composition is coarser than that of the natural profile, especially in the ash layer, where a large number of sand grains were produced by ancient humans using fire, and its content reached the highest value of 293.99 g kg^{-1}, much higher than the maximum value of the natural profile. However, in the cultural layer, the content of clay grains reaches a great value, and it is hypothesized that ancient human habitation activities increased the content of clay grains. The ratio of the mean value of χlf between the cultural and natural profiles is 1.15, and the ratio of the coefficient of variation is 1.96. It can be seen that the degree of variation of χlf in the cultural profile is greater than that in the natural profile, and the value is larger than that in the natural profile, especially in the ash and cultural layers, which reached 300.72 × 10^{-8} m^3 kg^{-1} and 231.06 × 10^{-8} m^3 kg^{-1}, respectively, and an anomalous maximum value of 705.51 × 10^{-8} m^3 kg^{-1} appeared in cultural layer 3. It is hypothesized that the increase in the content of soil magnetic material was caused by the activities of ancient human beings, such as using fire and living. Comparing the clay mineral types of the two profiles, the more obvious difference is in the transition layer of the natural profile, where the clay mineral type is a mixture of illite, montmorillonite, kaolinite, and chlorite, while the clay mineral types of the corresponding cultural layer 3 in the same period are illite and kaolinite, which indicated that the clay mineral types had become relatively homogeneous due to the disturbance of paleoanthropogenic activities.

4.2 Impact of soil development

Although farming activities promoted the decomposition of coarse soil particles into fine particles, the primitive farming technique of slash-and-burn cultivation produced a large amount

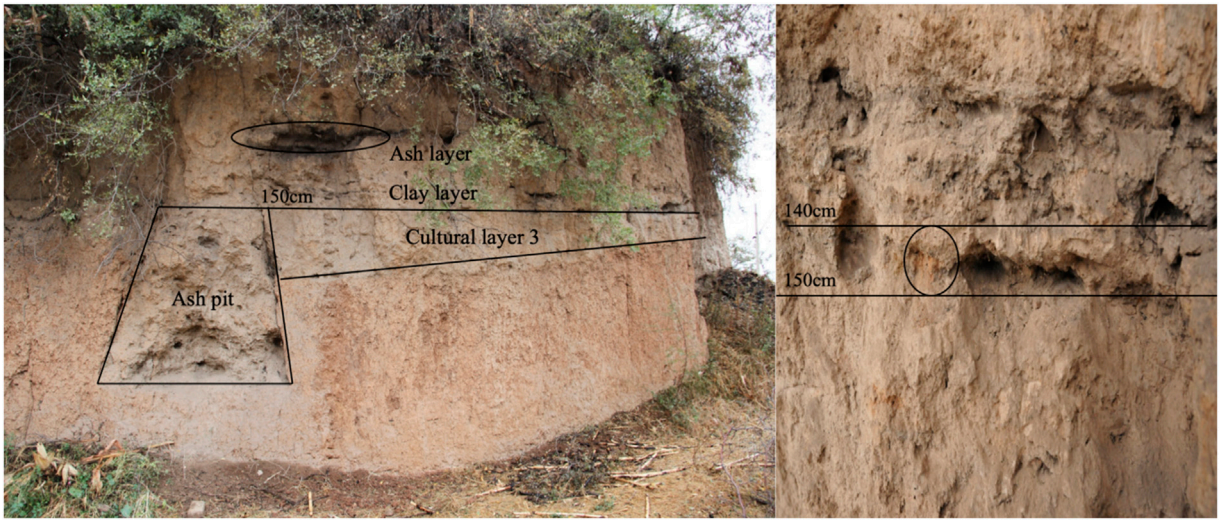

FIGURE 10
Clay layer in the cultural profile.

of ash and formed an ash layer with a very high sand content, which had a limited effect on promoting the development of the overall soil profile. Moreover, slash-and-burn farming mainly involves cutting down and burning forest trees without turning over the soil and practicing a farming system that leaves the land fallow after sowing seeds, which lacks turning, disturbing, and artificial ripening. Based on the soil development indicators, the inference is also further justified. By comparing the values of the developmental indicators in the cultural and natural profiles, the impact of paleoanthropogenic activities on soil development was investigated from a holistic perspective. In the cultural profile, the average values of Sa, Saf, and ba were 8.53, 15.94, and 0.22, respectively. On the other hand, in the natural profile, the average values were 7.94, 14.82, and 0.19, respectively. It can be found that the development indexes of the cultural profiles were all higher than those of the natural profiles, the degree of development of the natural profiles was higher than that of the cultural profiles, and the paleoanthropogenic activities in general hindered soil development. In addition, by comparing the values of the development indexes of the cultural layer with those of the topsoil and paleosoil layers within the cultural profile to explore the influence of paleo-human activities on soil development from a localized perspective, the average values of the development indexes of the cultural layer were 8.80, 16.44, and 0.23, respectively, while in the natural layer, they were 8.38, 15.66, and 0.21, respectively. It can be found that the development indexes of the cultural layer in the cultural profile were higher than those of the natural layer, the development of the cultural layer was weaker than that of the natural layer, and ancient human activities hindered the development of the soil layer.

One of the most obvious activities that hindered soil development was the hardening of the ground by ancient humans as a result of their habitation activities. In culture layer 2, kaolinite was found. According to the dating results, the climate was relatively dry and cold during this period, making it difficult for kaolinite to appear under natural conditions. Combined with field observations, a turbid orange clay layer (Figure 10) was found at the bottom of the layer (140–150 cm), with properties similar to those of the paleosoil. Combined with the soil particle size analysis, the clay content is high, and the dating data are abnormal, which is older than the paleosoil at the bottom. It is hypothesized that ancient humans carried the soil from other periods for covering grain or burying garbage and laid down the clay to achieve the effect of sealing. The magnetization value of this layer reaches an anomalous maximum, indicating that it has experienced fire baking and is presumed to have been hardened by fire. The soil layer that has been artificially compacted and baked, soil voids, and structure had suffered some damage, which had prevented the downward leaching or precipitation of soil particles and minerals to a certain extent, thus affecting soil development.

5 Conclusion

Ancient humans began their activities in the relatively low-lying area, in which farming activities led to an increase in the content of Gramineae and Quinoa in the soil, especially the appearance of phytosilicon bodies such as millet, corn, and rice, which confirms that ancient humans carried out primitive agricultural activities in this area. Slash-and-burn activities led to the filling of the soil with intruders such as charcoal chips and pottery shards, while at the same time, the coarse-grained texture was affected by the farming activities, which mostly decomposed into fine particles, and the content of sticky particles reached an extreme value. The total nitrogen, phosphorus, and calcium carbonate content exceeded the average value of the natural profile, indicating that ancient humans used human and animal excreta to fertilize the farmland.

The comparison of two typical profiles of the soil, under the influence of ancient human activities, macroscopically showed that the intruders in the soil body and morphological characteristics of the profile had obvious differences with the natural profile, and the macroscopically indicative features were mainly manifested in the presence of abundant relic remains. The microscopic indicative

features were mainly characterized by a sandy grain size composition, high χlf, and a relatively single clay mineral type.

Slash-and-burn cultivation not only produced a large amount of sand particles but also lacked soil tilling and artificial ripening, which had a limited effect on promoting the development of the soil. Through the analysis and comparison of the development indices of the cultural and natural profiles, it was found that ancient human activities hindered the development of the soil. In particular, the soil voids and structure of the ground created as a result of habitation activities were damaged to some extent, which prevented soil particles and minerals from leaching or precipitating downward to a certain extent, thus affecting soil development.

Data availability statement

The datasets presented in this study can be found in online repositories. The names of the repository/repositories and accession number(s) can be found in the article/Supplementary material.

Author contributions

LZ: methodology, project administration, supervision, validation, writing–review and editing, funding acquisition, and conceptualization. WW: methodology, project administration, validation, writing–review and editing, and conceptualization. JZ: formal analysis, software, validation, visualization, and writing–original draft. YS: formal analysis, validation, and writing–original draft. DC: validation and writing–original draft.

Funding

The author(s) declare that financial support was received for the research, authorship, and/or publication of this article. This research was funded by the National Natural Science Foundation of China (grant no. 41907001) and The Third Batch of Huizhi Leader Creative Space Project in Chengde Hi-Tech Zone (grant no. HZLC2024023).

Acknowledgments

This work was supported by the National Natural Science Foundation of China.

Conflict of interest

The authors declare that the research was conducted in the absence of any commercial or financial relationships that could be construed as a potential conflict of interest.

Publisher's note

All claims expressed in this article are solely those of the authors and do not necessarily represent those of their affiliated organizations, or those of the publisher, the editors, and the reviewers. Any product that may be evaluated in this article, or claim that may be made by its manufacturer, is not guaranteed or endorsed by the publisher.

References

Adam, P., Schaeffer, P., Schmitt, G., Bailly, L., Courel, B., Fresnais, M., et al. (2016). Identification and mode of formation of hopanoid nitriles in archaeological soils. *Org. Geochem.* 91, 100–108. doi:10.1016/j.orggeochem.2015.10.013

An, Z. (1988). Prehistoric agriculture in China. *Archaeol. J.* 4, 369–381.

Arnaud-fassetta, G., De Beaulieu, J. L., Suc, J. P., Provansal, M., Williamson, D., Leveau, P., et al. (2000). Evidence for an early land use in the rhone delta (mediterranean France) as recorded by late holocene fluvial paleoenvironments (1640–100 bc). *Geodin. Acta* 13 (6), 377–389. doi:10.1080/09853111.2000.11105381

Blasi, A., Politis, G., and Bayón, C. (2013). Palaeoenvironmental reconstruction of La Olla, a Holocene archaeological site in the Pampean coast (Argentina). *J. Archaeol. Sci.* 40 (3), 1554–1567. doi:10.1016/j.jas.2012.09.016

Brown, K. S., Marean, C. W., Herries, A. I. R., Jacobs, Z., Tribolo, C., Braun, D., et al. (2009). Fire as an engineering tool of early modern humans. *Science* 325 (5942), 859–862. doi:10.1126/science.1175028

Cao, Z., Yang, L., and Lin, X. (2007). Morphological characteristics of paddy fields, paddy soil profile, phytolith and fossil rice grain of the Neolithic Age in Yangtze River Delta. *Acta Pedol. Sin.* 44 (5), 838–847.

Carrancho, Á., and Villalaín, J. J. (2011). Different mechanisms of magnetisation recorded in experimental fires: archaeomagnetic implications. *Earth Planet. Sci. Lett.* 312 (1–2), 176–187. doi:10.1016/j.epsl.2011.10.006

Chang, K. C. (1967). The yale expedition to taiwan and southeast asian horticulture evolution. *Discovery* 11 (2), 3.

Chen, F., Xu, Q., Chen, J., Birks, H. J. B., Liu, J., Zhang, S., et al. (2015). East Asian summer monsoon precipitation variability since the last deglaciation. *Sci. Rep.* 5, 11186–11211. doi:10.1038/srep11186

Church, M. J., Peters, C., and Batt, C. M. (2007). Sourcing fire ash on archaeological sites in the Western and Northern Isles of Scotland, using mineral magnetism. *Geoarchaeology* 22 (7), 747–774. doi:10.1002/gea.20185

Cook, S. R., Clarke, A. S., Fulford, M. G., and Voss, J. (2014). Characterising the use of urban space: a geochemical case study from Calleva Atrebatum (Silchester, Hampshire, UK) Insula IX during the late first/early second century AD. *J. Archaeol. Sci.* 50 (1), 108–116. doi:10.1016/j.jas.2014.07.003

Cruz-y-Cruz, T., Sánchez, G., Sedov, S., Terrazas-Mata, A., Solleiro-Rebolledo, E., Tovar-Liceaga, R. E., et al. (2015). Spatial variability of Late Pleistocene-Early Holocene soil formation and its relation to early human paleoecology in Northwest Mexico. *Quat. Int.* 365, 135–149. doi:10.1016/j.quaint.2014.11.042

Dahms, D. E. (1998). Reconstructing paleoenvironments from ancient soils: a critical review. *Quat. Int.* 51, 58–60. doi:10.1016/s1040-6182(98)90222-1

Dirix, K., Muchez, P., Degryse, P., Kaptijn, E., MuŠič, B., Vassilieva, E., et al. (2013). Multi-element soil prospection aiding geophysical and archaeological survey on an archaeological site in suburban Sagalassos (SW-Turkey). *J. Archaeol. Sci.* 40 (7), 2961–2970. doi:10.1016/j.jas.2013.02.033

Dou, Y., Yang, S., Liu, Z., Clift, P. D., Yu, H., Berne, S., et al. (2010). Clay mineral evolution in the central Okinawa Trough since 28 ka: implications for sediment provenance and paleoenvironmental change. *Palaeogeogr. Palaeoclimatol. Palaeoecol.* 288 (1–4), 108–117. doi:10.1016/j.palaeo.2010.01.040

El Ouahabi, M., Hubert-Ferrari, A., and Fagel, N. (2017). Lacustrine clay mineral assemblages as a proxy for land-use and climate changes over the last 4 kyr: the Amik Lake case study, Southern Turkey. *Quat. Int.* 438, 15–29. doi:10.1016/j.quaint.2016.11.032

Fernández, F. G., Terry, R. E., Inomata, T., and Eberl, M. (2002). An ethnoarchaeological study of chemical residues in the floors and soils of Q'eqchi' maya houses at las pozas, Guatemala. *Geoarchaeology - An Int. J.* 17 (6), 487–519. doi:10.1002/gea.10026

Ferro-Vázquez, C., Martínez-Cortizas, A., Nóvoa-Muñoz, J. C., Ballesteros-Arias, P., and Criado-Boado, F. (2014). 1500 Years of soil use reconstructed from the chemical properties of a terraced soil sequence. *Quat. Int.* 346, 28–40. doi:10.1016/j.quaint.2014.03.023

Fleisher, J., and Sulas, F. (2015). Deciphering public spaces in urban contexts: geophysical survey, multi-element soil analysis, and artifact distributions at the 15th-16th-century AD Swahili settlement of Songo Mnara, Tanzania. *J. Archaeol. Sci.* 55, 55–70. doi:10.1016/j.jas.2014.12.020

Fredlund, G. G., and Tieszen, L. T. (1994). Modern phytolith assemblages from the north American great plains. *J. Biogeogr.*, 21(3), 321–335. doi:10.2307/2845533

Gallello, G., Pastor, A., Diez, A., La Roca, N., and Bernabeu, J. (2013). Anthropogenic units fingerprinted by REE in archaeological stratigraphy: mas d'Is (Spain) case. *J. Archaeol. Sci.* 40 (2), 799–809. doi:10.1016/j.jas.2012.10.005

Gerlach, R., Fischer, P., Eckmeier, E., and Hilgers, A. (2012). Buried dark soil horizons and archaeological features in the Neolithic settlement region of the Lower Rhine area, NW Germany: formation, geochemistry and chronostratigraphy. *Quat. Int.* 265, 191–204. doi:10.1016/j.quaint.2011.10.007

Haslam, M. (2004). The decomposition of starch grains in soils: implications for archaeological residue analyses. *J. Archaeol. Sci.* 31 (12), 1715–1734. doi:10.1016/j.jas.2004.05.006

Haslam, R., and Tibbett, M. (2004). Sampling and analyzing metals in soils for archaeological prospection: a critique. *Geoarchaeology An Int. J.* 19 (8), 731–751. doi:10.1002/gea.20022

Homburg, J. A., and Sandor, J. A. (2011). Anthropogenic effects on soil quality of ancient agricultural systems of the American Southwest. *Catena* 85 (2), 144–154. doi:10.1016/j.catena.2010.08.005

Kamenov, G. D., Brenner, M., and Tucker, J. L. (2009). Anthropogenic versus natural control on trace element and Sr-Nd-Pb isotope stratigraphy in peat sediments of southeast Florida (USA), ~1500 AD to present. *Geochimica Cosmochimica Acta* 73 (12), 3549–3567. doi:10.1016/j.gca.2009.03.017

Kelly, E. F., Chadwick, O. A., and Helinski, T. E. (1998). Kelly1998_Article_TheEffectOfPlantsOnMineralWeat.pdf. *Biogeochemistry* 42, 21–53. doi:10.1023/a:1005919306687

Kidder, T., Liu, H., Xu, Q., and Li, M. (2012). The alluvial geoarchaeology of the sanyangzhuang site on the Yellow River floodplain, henan Province, China. *Geoarchaeology* 27 (4), 324–343. doi:10.1002/gea.21411

Kim, J. C., Lee, Y.Il, Lim, H. S., and Yi, S. (2012). Geochemistry of quaternary sediments of the jeongokri archaeological site, korea: implications for provenance and palaeoenvironments during the late pleistocene. *J. Quat. Sci.* 27 (3), 260–268. doi:10.1002/jqs.1540

Knudson, K. J., Frink, L., Hoffman, B. W., and Price, T. D. (2004). Chemical characterization of Arctic soils: activity area analysis in contemporary Yup'Ik fish camps using ICP-AES. *J. Archaeol. Sci.* 31 (4), 443–456. doi:10.1016/j.jas.2003.09.011

Li, Y. (1980). An experimental exploration of the tools of production in primitive Chinese society. *Archaeology* 6, 515–520.

Linford, N. T., and Canti, M. G. (2001). Geophysical evidence for fires in antiquity: preliminary results from an experimental study. Paper given at the EGS XXIV General Assembly in The Hague, April 1999. *Archaeol. Prospect.* 8 (4), 211–225. doi:10.1002/arp.170

Lu, J., Hu, Z., Xu, Z., Cao, Z., Zhuang, S., Yang, L., et al. (2009). Effects of rice cropping intensity on soil nitrogen mineralization rate and potential in buried ancient paddy soils from the Neolithic age in China's Yangtze River delta. *J. Soils Sediments* 9 (6), 526–536. doi:10.1007/s11368-009-0138-1

Macphail, R. I. (2008). Soils and archaeology - science direct. *Encycl. Archaeol.*, 2064–2072.

Manalt, F., Beck, C., Disnar, J. R., Deconinck, J. F., and Recourt, P. (2001). Evolution of clay mineral assemblages and organic matte in the Late glacial-Holocene sedimentary infill of Lake Annecy (northwestern alps): paleoenvironmental implications. *J. Paleolimnol.* 25 (2), 179–192. doi:10.1023/A:1008140114714

Marcott, S. A., Marcott, S. A., Shakun, J. D., Clark, P. U., and Mix, A. C. (2013). A reconstruction of regional. 1198. doi:10.1126/science.1228026

Migliavacca, M., Pizzeghello, D., Ertani, A., and Nardi, S. (2013). Chemical analyses of archaeological sediments identified the ancient activity areas of an Iron age building at Rotzo (Vicenza, Italy). *Quat. Int.* 289, 101–112. doi:10.1016/j.quaint.2012.07.016

Neumann, K., Strömberg, C. A. E., Ball, T., Albert, R. M., Vrydaghs, L., and Cummings, L. S. (2019). International code for phytolith nomenclature (ICPN) 2.0. *Ann. Bot.* 124 (2), 189–199. doi:10.1093/aob/mcz064

Nielsen, N. H., and Kristiansen, S. M. (2014). Identifying ancient manuring: traditional phosphate vs. multi-element analysis of archaeological soil. *J. Archaeol. Sci.* 42 (1), 390–398. doi:10.1016/j.jas.2013.11.013

Oonk, S., Slomp, C. P., Huisman, D. J., and Vriend, S. P. (2009). Geochemical and mineralogical investigation of domestic archaeological soil features at the Tiel-Passewaaij site, The Netherlands. *J. Geochem. Explor.* 101 (2), 155–165. doi:10.1016/j.gexplo.2008.06.004

Parnell, J. J., Terry, R. E., and Nelson, Z. (2002). Soil chemical analysis applied as an interpretive tool for ancient human activities in Piedras Negras, Guatemala. *J. Archaeol. Sci.* 29 (4), 379–404. doi:10.1006/jasc.2002.0735

Pastor, A., Gallello, G., Cervera, M. L., and Guardia, M.De. (2016). Mineral soil composition interfacing archaeology and chemistry. *Trends Anal. Chem.* 78, 48–59. doi:10.1016/j.trac.2015.07.019

Paula, J., Mike, G. L., Warren, J., Chanda, J. H., Paul, G., Caitlin, E., et al. (2004). *IntCal04 terrestrial radiocarbon age calibration, 0-26 cal kyr BP Radiocarbon Publisher ' s PDF, also known as Version of record Publication date: 0–26.*

Peninsula, P. R. (1983). *Division s-5-soil genesis, morphology, and classification*, 1–7.

Salisbury, R. B. (2013). Interpolating geochemical patterning of activity zones at late neolithic and early copper age settlements in eastern Hungary. *J. Archaeol. Sci.* 40 (2), 926–934. doi:10.1016/j.jas.2012.10.009

Schlezinger, D. R., and Howes, B. L. (2000). Organic phosphorus and elemental ratios as indicators of prehistoric human occupation. *J. Archaeol. Sci.* 27 (6), 479–492. doi:10.1006/jasc.1999.0464

Shi, W., Zhu, C., and Xu, W. (2007). Relationship between abnormal phenomena of magnetic susceptibility curves of profiles and human activities at Zhongba Site in Chongqing. *ACTA Geogr. SINICA-CHINESE EDITION-* 62 (3), 267.

Shi, Y. F., Kong, Z. C., and Wang, S. M. (1992). Climate fluctuation and important events in Holocene warm period in China. *Sci. China Chem.* 22, 1300–1308.

Sitzia, L., Bertran, P., Boulogne, S., Brenet, M., Crassard, R., Delagnes, A., et al. (2012). The paleoenvironment and lithic taphonomy of Shi'Bat dihya 1, a middle paleolithic site in wadi surdud, Yemen. *Geoarchaeology* 27 (6), 471–491. doi:10.1002/gea.21419

Solís-Castillo, B., Solleiro-Rebolledo, E., Sedov, S., Liendo, R., Ortiz-Pérez, M., and López-Rivera, S. (2013). Paleoenvironment and human occupation in the maya lowlands of the usumacinta river, southern Mexico. *Geoarchaeology* 28 (3), 268–288. doi:10.1002/gea.21438

Stinchcomb, G. E., Messner, T. C., Stewart, R. M., and Driese, S. G. (2014). Estimating fluxes in anthropogenic lead using alluvial soil mass-balance geochemistry, geochronology and archaeology in eastern USA. *Anthropocene* 8 (2014), 25–38. doi:10.1016/j.ancene.2015.03.001

Suleimanov, R. R., and Obydennova, G. T. (2006). Soil-archaeological studies of the bronze-age settlement on the Urshak River floodplain, Bashkortostan. *Eurasian Soil Sci.* 39, 820–825. doi:10.1134/s1064229306080035

Sullivan, K. A., and Kealhofer, L. (2004). Identifying activity areas in archaeological soils from a colonial Virginia house lot using phytolith analysis and soil chemistry. *J. Archaeol. Sci.* 31 (12), 1659–1673. doi:10.1016/j.jas.2004.04.007

Terry, R. E., Fernández, F. G., Parnell, J. J., and Inomata, T. (2004). The story in the floors: chemical signatures of ancient and modern Maya activities at Aguateca, Guatemala. *J. Archaeol. Sci.* 31 (9), 1237–1250. doi:10.1016/j.jas.2004.03.017

Tsatskin, A., and Nadel, D. (2003). Formation processes at the Ohalo II submerged prehistoric campsite, Israel, inferred from soil micromorphology and magnetic susceptibility studies. *Geoarchaeology* 18 (4), 409–432. doi:10.1002/gea.10069

Turner, S., Graham, E., Macphail, R., Duncan, L., Rose, N. L., Yang, H., et al. (2021). Mercury enrichment in anthrosols and adjacent coastal sediments at a Classic Maya site, Marco Gonzalez, Belize. *Geoarchaeology* 36 (6), 875–896. doi:10.1002/gea.21868

Vittori Antisari, L., Cremonini, S., Desantis, P., Calastri, C., and Vianello, G. (2013). Chemical characterisation of anthro-technosols from bronze to middle age in bologna (Italy). *J. Archaeol. Sci.* 40 (10), 3660–3671. doi:10.1016/j.jas.2013.04.023

Walkington, H. (2010). Soil science applications in archaeological contexts: a review of key challenges. *Earth-Science Rev.* 103 (3–4), 122–134. doi:10.1016/j.earscirev.2010.09.002

Wang, J., Li, A., Xu, K., Zheng, X., and Huang, J. (2015). Clay mineral and grain size studies of sediment provenances and paleoenvironment evolution in the middle Okinawa trough since 17ka. *Mar. Geol.* 366, 49–61. doi:10.1016/j.margeo.2015.04.007

Wang, X., Fuller, B. T., Zhang, P., Hu, S., Hu, Y., and Shang, X. (2018). Millet manuring as a driving force for the Late Neolithic agricultural expansion of north China. *Sci. Rep.* 8 (1), 5552–5610. doi:10.1038/s41598-018-23315-4

Wells, E. C. (2004). Investigating activity patterns in Prehispanic plazas: weak acid-extraction ICP–AES analysis of anthrosols at classic period El Coyote, Northwestern Honduras. *Archaeometry* 46 (1), 67–84. doi:10.1111/j.1475-4754.2004.00144.x

Wilson, C. A., Davidson, D. A., and Cresser, M. S. (2008). Multi-element soil analysis: an assessment of its potential as an aid to archaeological interpretation. *J. Archaeol. Sci.* 35 (2), 412–424. doi:10.1016/j.jas.2007.04.006

Wu, K., Li, L., Ju, B., and Chen, J. (2019). Soil Series of China (He nan). *China Sci. Publ.*

Yan, W. (1989). *Yangshao culture research*. Beijing: Cultural Relics Publishing House.

Zgłobicki, W. (2013). Impact of microtopography on the geochemistry of soils within archaeological sites in SE Poland. *Environ. Earth Sci.* 70 (7), 3085–3092. doi:10.1007/s12665-013-2368-1

Zha, L., Wu, K., Liang, S., and Zhuang, D. (2020). Study on physical and chemical characteristics of soil and reconstructing the paleoenvironment of an archaeological site at the Yangshao, village. *Ecol. Environ. Sci.* 29 (6), 1268–1276. doi:10.16258/j.cnki.1674-5906.2020.06.024

Zhang, Y., Guo, Z., Deng, C., Zhang, S., Wu, H., Zhang, C., et al. (2014). The use of fire at Zhoukoudian: evidence from magnetic susceptibility and color measurements. *Chin. Sci. Bull.* 59 (10), 1013–1020. doi:10.1007/s11434-013-0111-7

Zhong, H., and Zhao, Z. (2023). A preliminary study of agricultural production patterns in the central plains during the late Yangshao culture period. *Agric. Hist. China* 02, 52–61.